Economic Geology
Vol. 76, 1981, pp. 637–647

Remote Detection of Geobotanical Anomalies Related to Porphyry Copper Mineralization

RICHARD W. BIRNIE AND JOSEPH R. FRANCICA

Department of Earth Sciences, Dartmouth College, Hanover, New Hampshire 03755

Abstract

Visible and near infrared (450–1,000 nm) reflected radiance spectra of the ground cover vegetation were measured at the Mesatchee Creek porphyry copper prospect in Washington. The reflected radiance data are integrated over 400-m^2 surfaces of a forest dominated by Douglas fir with lesser amounts of western larch. Analysis of the reflected radiance data indicates that the spectra from within the pyrite halo of the deposit have anomalously high reflected radiance values at 565 nm and low reflected radiance values at 465 nm. Six flight lines were flown on each of two days. Taking one flight line from the first day's data as the control line, individual spectra with a 565 nm/465 nm reflected radiance ratio value greater than 1.7 fall predominantly within the pyrite halo. When this threshold value is applied to all flight lines from the first day, 36.8 percent of the spectra within the pyrite halo and 5.4 percent of the spectra outside the pyrite halo are classified as anomalous. The zone of mineralization is clearly defined by the cluster of anomalous spectra. There is an 87 percent probability of an anomalous spectrum lying within the mineralized zone. The same technique was applied to the second day's data. The threshold ratio value was optimized at 1.6 and the resultant probability of an anomalous spectrum lying within the mineralized zone is then 92 percent. Higher cutoffs improve the probability of an anomalous spectrum falling in the mineralized zone; but fewer spectra are classified as anomalous and the extent of the mineralized zone is not as well defined. The geobotanical anomaly correlates with the pyrite halo and is not preferentially concentrated within the high Cu soil geochemical zones. Comparison with results obtained in lodgepole pine areas at Heddleston, Montana, shows that different vegetation types manifest geobotanical anomalies in different spectral regions.

Introduction

VEGETATION has been used as a guide to subsurface geology and mineralization for centuries. Within present-day scientific disciplines, there are two fields of study based on these vegetation indicators: biogeochemistry and geobotany.

Investigators in the field of biogeochemistry analyze plant matter to detect the uptake of heavy metals. Anomalous concentrations of heavy metals in the leaves, needles, or twigs of vegetation often correlate with subsurface geochemical anomalies. Applications of biogeochemistry to mineral exploration are discussed by Rose et al. (1979), Girling et al. (1979), Brooks (1972), and NASA (1968).

The field of geobotany involves the identification of particular plant species whose growth is restricted to definable geologic or soil environments. There are many indicator plants that are known to grow only in soils containing large amounts of particular heavy metals (Carlisle and Cleveland, 1958; Cannon, 1960, 1971; Brooks, 1972; and Rose et al., 1979). In addition, geobotanical studies may detect density, morphological, or color changes within a given species of vegetation. These changes may take the form of gigantism, dwarfing, or chlorosis (yellow discoloration) (Yost and Wenderoth, 1971; Reynolds et al., 1973). This effect on the vigor of the vegetation may or may not correlate with a biogeochemical anomaly in the plant matter. For example, the color anomalies in lodgepole pine related to porphyry copper mineralization in Montana (Birnie and Dykstra, 1978) were not associated with a biogeochemical pattern, but the color differences noted in lichen related to copper mineralization in California do correlate with a biogeochemical uptake of Cu by the lichen (Czehura, 1977).

This paper deals with a method of detecting geobotanical anomalies using an airborne remote sensing technique. Similar experiments have been undertaken at other sites, and these are briefly described by Birnie and Hutton (1976), Collins et al. (1977, 1978), and Birnie and Dykstra (1978). With the advent of satellite and airborne remote sensors that are capable of measuring reflected solar radiance values (intensity of sunlight reflected by the surface over a range of wavelengths), new techniques have become available for mineral prospecting. These techniques involve correlating surface reflected radiance anomalies with mineralization. These anomalies may directly manifest mineralization, as with iron oxide-stained bedrock outcrops, or they may indirectly

manifest the mineralization, as in the case of geobotanical anomalies.

Numerous studies have employed remote sensors, principally the Landsat satellites, to detect color anomalies associated with mineralized zones in regions completely devoid of vegetation (for example: Rowan et al., 1974; Schmidt, 1975; Schmidt and Bernstein, 1977; Collins, 1978a; Dykstra and Birnie, 1979). These studies were conducted in arid regions of Nevada and Pakistan where vegetative cover is minimal and where the bed rock is exposed at the surface and within "sight" of the remote sensor.

A geobotanical anomaly must be sufficiently large, both spatially and spectrally, to be detected by airborne or satellite techniques. Bølviken et al. (1977) detected naturally Cu-poisoned vegetation stands on enhanced color ratio images of Landsat digital data. However, since many geobotanical anomalies are very subtle and not visible to the unaided eye, satellite imagery and conventional remote sensing techniques such as air photo interpretation have not been entirely satisfactory.

Previous work of other investigators who undertook careful land- and laboratory-based studies indicates that there are anomalous spectral reflectance properties in the vegetation growing in mineralized zones. Notable among these studies are those of Canney et al. (1970), Yost and Wenderoth (1971), Howard et al. (1971), Press (1974), and Lyon (1975). Working in various geologic settings, as porphyry Cu-Mo, vein Cu, vein Pb-Zn, and skarn Mo, these investigators reported that there are detectable spectral differences in the vegetation growing in mineralized areas. The vegetation types include red spruce, fir balsam, ponderosa pine, cork oak, juniper, and pinion pine. The restricted areal coverage of these studies and the time and effort required for individual spectral measurements make them unsuitable for an exploration program. For instance, the cherry picker measurements made by Yost and Wenderoth (1971) would be impossible in areas of poor access for a large truck. However, these studies do indicate that there are geobotanical anomalies associated with mineralized zones and that these geobotanical anomalies are manifested by anomalous reflectance properties of the vegetation.

In cooperation with colleagues at the NASA Goddard Institute for Space Studies (GISS) in New York, we have developed a simple procedure for the analysis of reflected radiance data that can be collected rapidly over a large area and used in an exploration program.

Instrumentation and Reflectance Properties of Vegetation

The airborne spectroradiometer used in this study was assembled at GISS by Chiu and Collins (1978). The instrument, which measures the reflected radiance ($mW \cdot cm^{-2} \cdot sr^{-1}$) in the visible and near infrared wavelengths of the electromagnetic spectrum (430–1,000 nm), has a spectral band width per channel of 1.4 nm. The instrument is mounted in a light airplane and flown at an elevation of 600 m above the ground. The reflected radiance is integrated over a surface area about 20 m on a side. Photographs, which are taken every ten spectra, permit correlation of the spectra with the ground. The instrument is calibrated in the laboratory to reflected radiance values by means of a standard tungsten lamp.

Individual spectra are plots of reflected radiance ($mW \cdot cm^{-2} \cdot sr^{-1} \cdot ch^{-1}$) vs. wavelength (nm). Figure 1 shows a typical spectrum for a Douglas fir canopy. Relatively low reflected radiance values in the visible portion of the spectrum (430–700 nm) are due to strong absorption by chlorophyll in the needles. The chlorophyll absorption, which is strongest at approximately 420 and 665 nm, drops off in the 560-nm region; this accounts for the green appearance of vegetation. The near infrared (700–1,000 nm) reflected radiance values are much higher than the visible because there are no strong absorption bands in this region. Knipling (1970) gives a detailed discussion of the visible and near infrared reflectance properties of vegetation. The narrow absorption band manifesting itself as a steep-sided trough centered at 760 nm (Fig. 1) is due to absorption by oxygen in the atmosphere. The narrow absorption trough at 720 nm and the broad absorption bands at 820 and 940 nm are due to absorption by water vapor in the atmosphere. Fraser et al. (1975) discuss the interaction of radiation with the atmosphere.

General Geology and Vegetation Cover

The Mesatchee Creek porphyry copper deposit in Washington was chosen for this study. The deposit

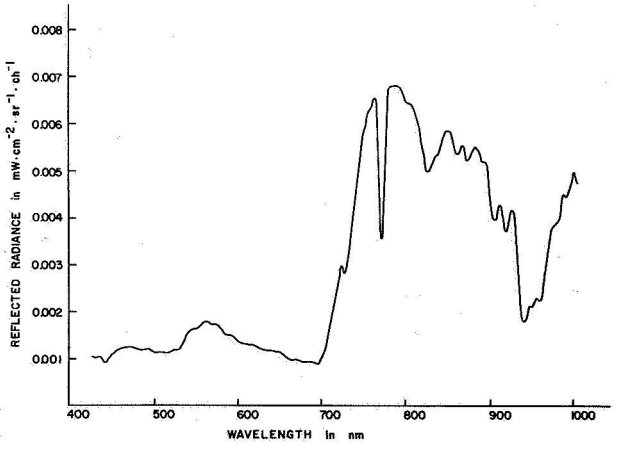

FIG. 1. A generalized reflected radiance spectrum of Douglas fir trees.

is located on Washington State Highway 410 about 87 km northwest of Yakima, Washington, and is centered at the confluence of the American River and Mesatchee Creek (Figs. 2 and 3). Although the maximum relief in the area included in Figures 2 and 3 is about 740 m, the flight lines were chosen to coincide with the flatter areas that have a maximum relief of about 200 m. The region is covered in the 1:62,500 Bumping Lake, Washington, U. S. Geological Survey topographic map. Numerous mining claims and small-scale workings have existed in the area since the 1890s (Simmons et al., 1974). The geology and soil geochemistry of the study area have been mapped in detail by Duval International who provided us with their data (Fig. 2).

This deposit is one of the Cascade Province porphyry copper deposits which are noted for their distinctive mineralogy, metallogeny, and time distribution (Hollister, 1978). The mineralization is located at the contact of Tertiary volcanic rocks of the Ohanapecosh Formation and a group of Tertiary quartz monzonite, quartz diorite, diorite, and quartz porphyry intrusives (Fig. 2). Sulfide mineralization is predominantly pyrite and chalcopyrite with some secondary chalcocite (Simmons et al., 1974). Tungsten in the form of scheelite also occurs with the sulfides (Hollister, 1978). The 6.2-m.y. K-Ar date of the hydrothermal sericite makes Mesatchee Creek the youngest of the Cascade porphyries (Hollister, 1978).

A preliminary stream sediment geochemical survey by Moen (1969) was followed by grab and chip rock analyses by Simmons et al. (1974). Duval International staked claims in the area and, in 1973, undertook a field program including drilling, a magnetometer survey, and a soil geochemical study (Fig. 2).

The principle vegetation stand over the Mesatchee Creek deposit is mature Douglas fir (*Pseudotsuga menziesii*). This species typically forms dense pure stands with individual trees over 30 m high. The needles form rows on opposite sides of the twig, are 3 to 3 cm long, and are about 1.5 mm wide. Lesser amounts of western larch (*Larix occidentalis*), which is commonly associated with Douglas fir east of the Cascade divide (Franklin and Dyrness, 1973; Mosher and Lunnum, 1974), are scattered through the forest. A dense stand of larch occurs in the low land just to the west of the swamps which line up along the American River (Fig. 3). The larches grow over 40 m high with needles 2.5 to 3.5 cm long. Both species

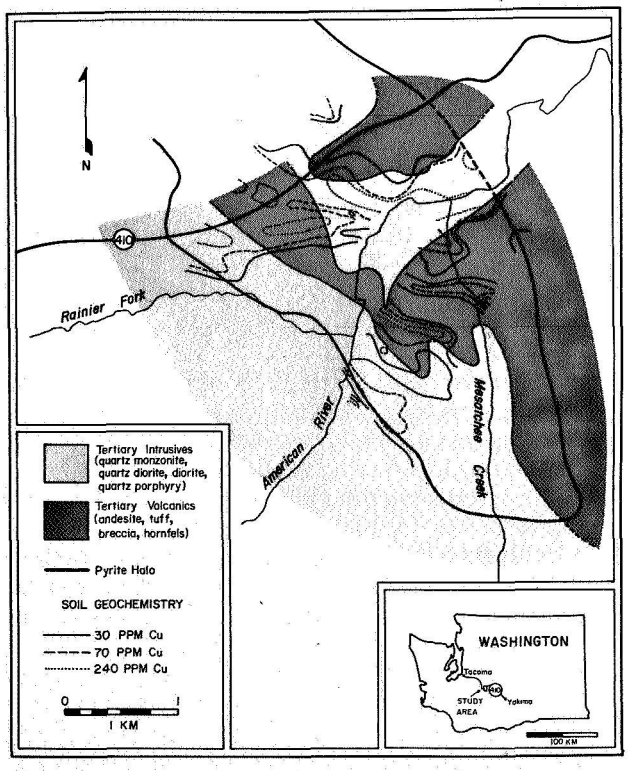

FIG. 2. Generalized geologic, soil geochemical, and pyrite halo map of the Mesatchee Creek prospect (after map provided by Duval International). Location of the area in Washington State is indicated in the inset.

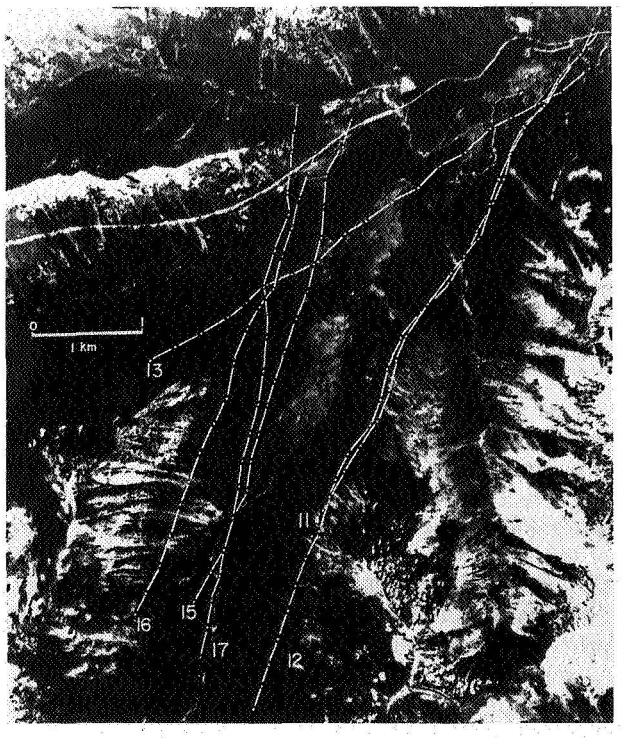

FIG. 3. Vertical air photo of Mesatchee Creek prospect. Washington State Highway 410 crosses photo at top in a nearly east-west direction. Area covered corresponds approximately to that of Figure 2. Lines flown on September 25, 1978, are indicated with dots representing the centers of photos shot every ten spectra. (Photo shot July 13, 1978, scene ID 5780026334134, frame #4143, original scale 1/128, 727.)

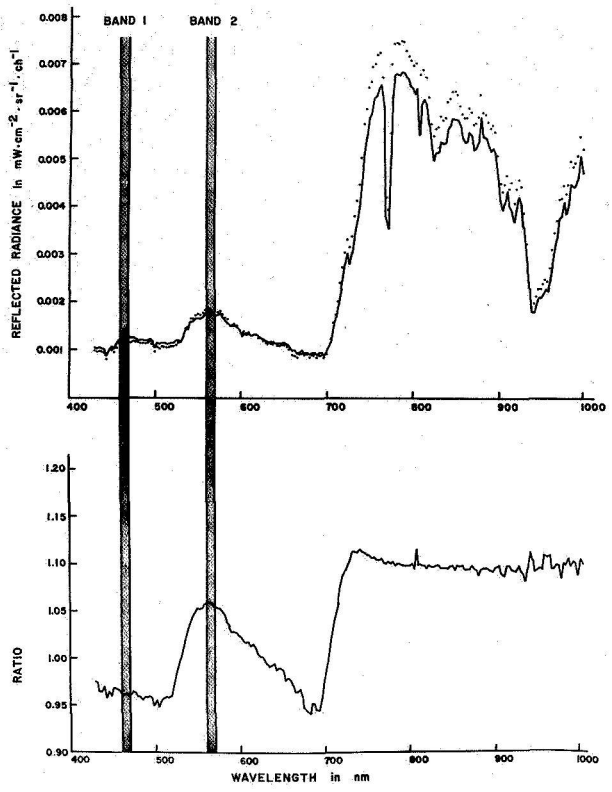

FIG. 4. (Top). Average of the mineralized (dotted line) and nonmineralized (solid line) reflected radiance spectra from one flight line. (Bottom). Channel by channel ratio of reflected radiance value of mineralized to nonmineralized spectra shown above. Vertical shaded bars indicate spectral regions used for classification.

require full sunlight and produce a dense canopy cover. For a more detailed description of the forest in the area, refer to Mosher and Lunnum (1974), Franklin and Dyrness (1973), and the U. S. Department of Agriculture Forest Service Tri-Ecoclass Subsystem map, compartment numbers 8410 and 8411.

Results

A series of six flight lines were flown on each of two days: approximately 11:00 a.m. on September 25, 1978, and approximately 1:00 p.m. on September 26, 1978. These flight lines were chosen to cover as much of the densely forested mineralized zone as possible and to minimize topographic variation within each flight line. The soil geochemistry and pyrite halo map provided by Duval International (Fig. 2) served as a guide for locating the mineralized zone. The line of swamps striking northeast through the center of the deposit (Fig. 3) corresponds to the zone where there are no soil geochemical data.

Photos are taken every ten spectra along the flight lines. These photos permit precise location of the flight lines and individual spectra. Each flight line covers 4 to 7 km and includes about 250 spectra. Each spectrum represents the reflected radiance integrated over a square about 20 m on a side. The ground surface corresponding to each spectrum was checked on the photos, and spectra not covering densely forested areas were removed from consideration. For example, parts of flight line 13 (Fig. 5) and flight line 21 (Fig. 6) were over the swamps and these spectra were removed from consideration. Generally, about 5 to 10 percent of the spectra in any flight line are removed because they cover roads, streams, swamps, sparse forest stands, or rock outcrops. However, there may be subtle changes in the density of the canopy that are not accounted for by these obvious features, and these will influence the reflected radiance data by increasing the contribution of the ground and undercover and decreasing the contribution of the tree canopy to the spectrum.

The first part of the experiment tested whether the spectroradiometer was able to detect a unique spectral response from the vegetated surface in the mineralized zone. The mineralized zone was initially defined as the region within the 70-ppm Cu soil geochemical anomaly (Fig. 2). Spectra were considered nonmineralized if they occurred outside the 30-ppm Cu contour. Spectra falling in the region between the 30- and 70-ppm contours were omitted from this initial test, because they fall in the intermediate region, neither distinctly mineralized nor distinctly nonmineralized. For each flight line, all spectra from within the mineralized zone were averaged. The resultant average spectrum represents an average of about 40 mineralized spectra and was compared to the average of the nonmineralized spectra. An example of these averaged spectra for one flight line is given in the top of Figure 4. The mineralized spectrum shows slightly increased reflected radiance at 565 nm (green) and slightly decreased reflected radiance at 465 nm (blue). The two spectra in Figure 4 show differences at 670 nm (red) and at wavelengths greater than 700 nm (near infrared); however, reference to similar pairs of averaged spectra from the 11 other flight lines showed that these differences were not consistent and varied between flight lines.

The comparison of the two averaged spectral plots is facilitated by performing a channel by channel ratio of their reflected radiance values. The bottom of Figure 4 is a ratio plot of the mineralized/nonmineralized spectra. The peak at 565 nm emphasizes the approximately 5 percent higher reflected radiance value of the mineralized spectrum at that wavelength.

On the basis of this ratio plot (Fig. 4) and those of the other 11 flight lines, it was determined that the geobotanical anomaly at Mesatchee Creek manifests itself by relatively high reflected radiance at 565 nm and relatively low reflected radiance at 465 nm. De-

spite the range of spectral data between 430 and 1,000 nm, only two relatively narrow bands of data need be analyzed. These bands are defined as band 1 (B1) between 460 and 470 nm and band 2 (B2) between 560 and 570 nm (Fig. 4). The 10-nm spectral width of these bands is much narrower than the 100-nm minimum band width on the Landsat satellite. The need for narrow spectral band widths for analyzing types of vegetation including wheat and alfalfa has been noted by Collins (1978b) and Collins et al. (1977).

For spectral measurements of this sort to be a useful exploration tool, a method of analyzing individual spectra, without prior knowledge of their state of mineralization, must be devised. The previous discussion indicates that the mineralized spectra are relatively "greener" than the nonmineralized spectra. A band 2/band 1 (B2/B1) ratio value for an individual spectrum is a measure of this "greening." The likelihood of an individual spectrum being mineralized increases with its B2/B1 ratio value.

For the spectral data collected on September 25, 1978, flight line 11 was chosen as the control line. The B2/B1 ratio was calculated for all spectra along this flight line. By correlating the B2/B1 ratio value with the ground truth, it was determined that spectra with a value greater than 1.7 clustered within the mineralized zone. Spectra with B2/B1 values less than 1.7 clustered outside the mineralized zone. This ratio threshold was then applied to all flight lines on September 25. The results of this analysis are plotted in Figure 5, where anomalous spectra with a B2/B1 ratio greater than 1.7 are indicated by dots, and background spectra are left blank. It is clear that there is a concentration of anomalous spectra over the mineralized zone and that there is a paucity of anomalous spectra outside the mineralized zone.

The results can be analyzed quantitatively considering the area within the 30-ppm Cu soil geochemical contour (Fig. 2) as the mineralized zone and the target for a successful classification (Table 1). Background values outside the mineralized zone are generally less than 20-ppm Cu. Of the six flight lines flown on September 25, there are 301 spectra that lie within the greater than 30-ppm Cu soil geochemical zone. Of these 301 spectra, 110 have B2/B1 ratio values greater than 1.7 and were classified as anomalous. The density of anomalous spectra within the high copper zone is, therefore, 36.5 percent (Table 1). Outside the high copper zone there are 813 spectra, and 77 were classified as anomalous. The density of anomalous spectra outside the high copper zone is, therefore, 9.5 percent. These 77 spectra represent errors of commission.

An indicator of the degree to which anomalous spectra are concentrated inside the mineralized zone can be calculated by dividing the density (%) of anomalous spectra within the mineralized zone by the sum of the densities (%) of anomalous spectra within and outside the mineralized zone (36.5/(36.5+9.5) = 79%). This is a measure of the probability of an anomalous spectrum falling within the mineralized zone and, because it contrasts the density of anomalous spectra, not the total number of anomalous spectra; it is independent of the relative lengths of the flight line segments over mineralized and nonmineralized ground. Hence, when employing the 1.7 B2/B1 cutoff, there is a 79 percent probability that an anomalous spectrum occurs within the mineralized zone.

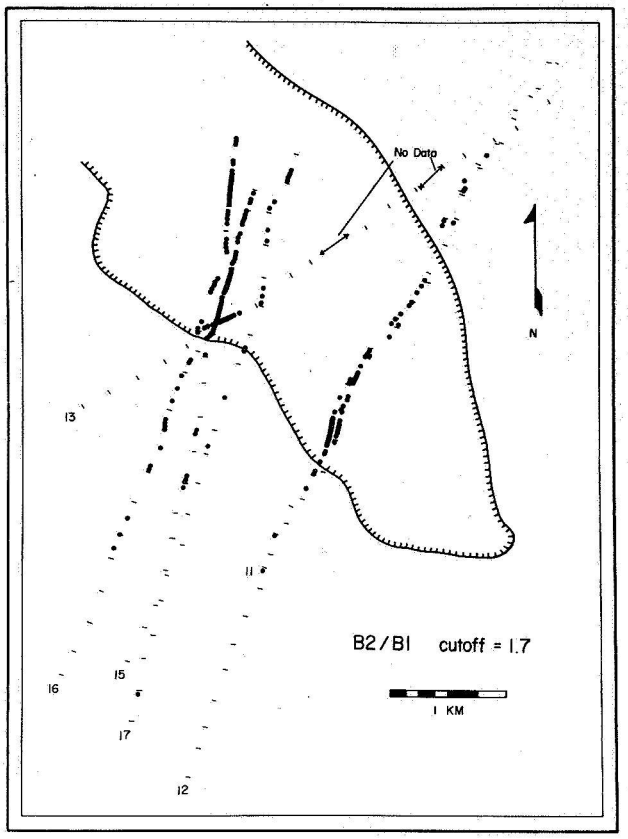

FIG. 5. Plot of anomalous spectra (dots) based on B2/B1 cutoff = 1.7 for data of September 25, 1978. The pyrite halo is indicated by the hatched line; the dashes represent centers of photos taken every 10 spectra; spectra not classified anomalous are left blank.

The anomalous spectra are not unique to the high Cu soil geochemical zone but are characteristic of the zone within the pyrite halo which includes more area than the high Cu zone (Figs. 2 and 5). If the target for a successful classification is redefined to include those spectra that fall within the pyrite halo, the ability to discriminate is improved (Table 1). There are 394 spectra within the pyrite halo; 145 of these are classified as mineralized. The density of mineralized

TABLE 1. Results of September 25, 1978, Survey

	Target = High Cu soil geochemical anomaly				Target = Pyrite halo			
	Percent of spectra classified anomalous				Percent of spectra classified anomalous			
Anomaly cutoff (B2-B1 ratio)	Within target (total = 301)	Outside target (total = 813)	Probability (%)*	χ^2†	Within target (total = 394)	Outside target (total = 720)	Probability (%)*	χ^2†
2.0	3.3	1.0	77	7.6	4.6	0	100	33.4
1.9	7.3	2.1	78	17.7	9.1	0.4	96	57.3
1.8	20.3	4.2	83	72.8	21.8	1.0	96	144.8
1.7	36.5	9.5	79	115.3	36.8	5.4	87	181.9
1.6	57.1	21.0	73	134.4	57.3	16.3	78	202.0
1.5	75.1	39.4	66	112.2	78.2	33.1	70	207.4
1.4	84.7	57.9	59	69.4	89.1	52.1	63	153.6
1.3	94.7	74.9	56	54.2	97.2	71.0	58	110.6

* Probability of anomalous spectrum falling within target calculated by dividing percent within target by sum of percent within plus percent outside (see text)

† Based on the calculated χ^2 statistic, the probabilities that the pattern of anamalous spectra is random are as follows: P ($0.46 < \chi^2 < \infty$) = 0.50; P ($2.7 < \chi^2 < \infty$) = 0.10; P ($6.6 < \chi^2 < \infty$) = 0.01; P ($10.8 < \chi^2 < \infty$) = 0.001

spectra within the pyrite halo is 36.8 percent. Hence, the density of mineralized spectra within the pyrite halo is equivalent to that within the high copper zone. We conclude that the factor producing the geobotanical anomaly is not uniquely restricted to the high Cu geochemical zone but is controlled by the pyrite halo. Also, by defining the mineralized zone as all spectra within the pyrite halo, many of the spectra that were considered errors of commission by the previous analysis now become successful classifications. There are 720 spectra outside the pyrite halo, 39 of these are classified as mineralized, and the density of errors of commission is reduced to 5.4 percent. The overall probability of an anomalous spectrum lying within the pyrite halo is 87 percent.

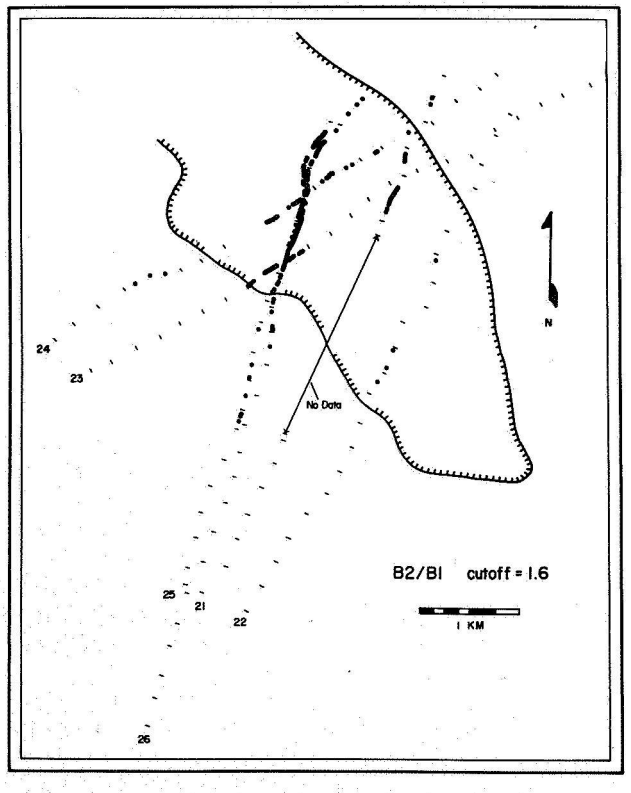

FIG. 6. Plot of anomalous spectra (dots) based on B2/B1 cutoff = 1.6 for data of September 26, 1978. Symbols same as in Figure 5.

The same method of analysis was applied to the September 26, 1978, data. Flight line 21 was used as the control line and a 1.6 B2/B1 ratio value was judged optimum for isolating the mineralized zone. The results of this analysis are plotted (Fig. 6) and tabulated in Table 2. Qualitatively the results are very similar to those of the previous day. The easternmost flight lines do not define the mineralized zone as well as the previous day, but the western set of flight lines defines the zone very well. Note in Table 2 that for a 1.6 cutoff the density of mineralized spectra within the high copper zone is 26 percent which is similar to the 31 percent value within the pyrite halo. This supports the observation that the geobotanical anomaly is related not uniquely to the high copper zone but includes all the area within the pyrite halo. For the second day's data with a 1.6 B2/B1 cutoff, the overall probability of an anomalous spectrum lying within the pyrite halo is 92 percent.

The correlation of spectra with high B2/B1 ratio values with the mineralized zone is emphasized further by examining the classification results using different B2/B1 cutoffs. In Figure 7, the classification results are plotted for 1.6, 1.7, 1.8, and 1.9 B2/B1

TABLE 2. Results of September 26, 1978, Survey

Anomaly cutoff (B2-B1 ratio)	Target = High Cu soil geochemical anomaly: Percent of spectra classified anomalous, Within target (total = 338)	Outside target (total = 865)	Probability (%)*	χ^2†	Target = Pyrite halo: Percent of spectra classified anomalous, Within target (total = 447)	Outside target (total = 756)	Probability (%)*	χ^2†
2.0	0.3	0.1	75	0.5	0.4	0	100	3.4
1.9	1.5	0.5	75	3.4	2	0	100	15.3
1.8	5.6	1.6	78	14.6	6.9	0.1	99	50.2
1.7	15.3	3.0	84	61.4	17.0	0.3	98	129.8
1.6	26.3	8.1	76	70.5	31.1	2.6	92	198.2
1.5	41.1	17.1	71	77.2	47.4	9.9	83	217.5
1.4	56.8	33.4	63	55.4	64.2	25.7	71	173.9
1.3	70.4	52.6	57	31.6	77.0	46.2	63	109.1

* Probability of anomalous spectrum falling within target calculated by dividing percent within target by sum of percent within plus percent outside (see text)

† Based on the calculated χ^2 statistic, the probabilities that the pattern of anamalous spectra is random are as follows: P ($0.46 < \chi^2 < \infty$) = 0.50; P ($2.7 < \chi^2 < \infty$) = 0.10; P ($6.6 < \chi^2 < \infty$) = 0.01; P ($10.8 < \chi^2 < \infty$) = 0.001.

cutoffs for the September 25, 1978, data. Although all four maps contain a concentration of anomalous spectra within the mineralized zone, the probability of a successful classification increases with the cutoff value (Table 1 and Fig. 8). Anomalous spectra in the 1.9 cutoff map have a 96 percent probability of falling within the pyrite halo. While this high cutoff value locates the general region of the pyrite halo, the lower cutoff values better define the limits of the pyrite halo. The better definition of the limits of the pyrite halo comes at the expense of greater errors of commission.

The probability of an anomalous spectrum falling within the pyrite halo is plotted against a range of B2/B1 cutoff values in Figure 8. At a cutoff value of 1.3, there is a slightly better than 50/50 chance of an anomalous spectrum falling within the pyrite halo, but the probability increases rapidly as the cutoff is raised.

Data for all the cutoff values tabulated in Tables 1 and 2 support the observation that the density of anomalous spectra within the high soil Cu zone is always about the same as the density of anomalous spectra within the pyrite halo.

Another means of quantifying the success of the B2/B1 cutoff in discriminating the mineralized zone is the χ^2 statistic. In this case, the χ^2 statistic is a measure of the degree to which the distribution of anomalous spectra is random with respect to mineralization. This statistic has been calculated for all B2/B1 cutoff values in both days (Tables 1 and 2). Most all flight lines show less than a 0.1 percent probability that the pattern of anomalous spectra is random.

In an exploration program, there may not be an opportunity to use a control flight line to determine the optimum B2/B1 cutoff value to define the mineralized zone. In this case, a series of cutoff maps like those of Figure 7 should be prepared. The highest cutoff value maps will show very few anomalous spectra, but these anomalous spectra have the highest probability of being mineralized. Lower cutoff value maps can be studied to determine the extent of mineralization in the high probability targets and to identify other targets of lower probability.

Discussion and Conclusions

Within the complex interactions of the forest ecosystem, there are many botanical factors that could affect the reflectance properties of the plant canopy and produce the anomalous B2/B1 ratio which we observe to correlate with the mineralization. A major factor in determining the reflectance properties of a plant canopy is the degree to which incident solar radiation is absorbed by plant pigments, particularly chlorophyll. Changes in pigment absorption have been observed in laboratory experiments on several plant types grown in soils doped with several heavy metals (Press and Norman, 1972; Chang and Collins, 1980; Horler et al., 1980). Collins et al. (1977, 1978) report remotely detected pigment absorption differences in vegetation that correlate with soil geochemical anomalies.

Since the spectroradiometer integrates the reflected radiance over 20-m squares, we feel that at Mesatchee Creek other factors might contribute to the anomaly. One possible factor is a change in the density of the vegetation over the mineralized zone.

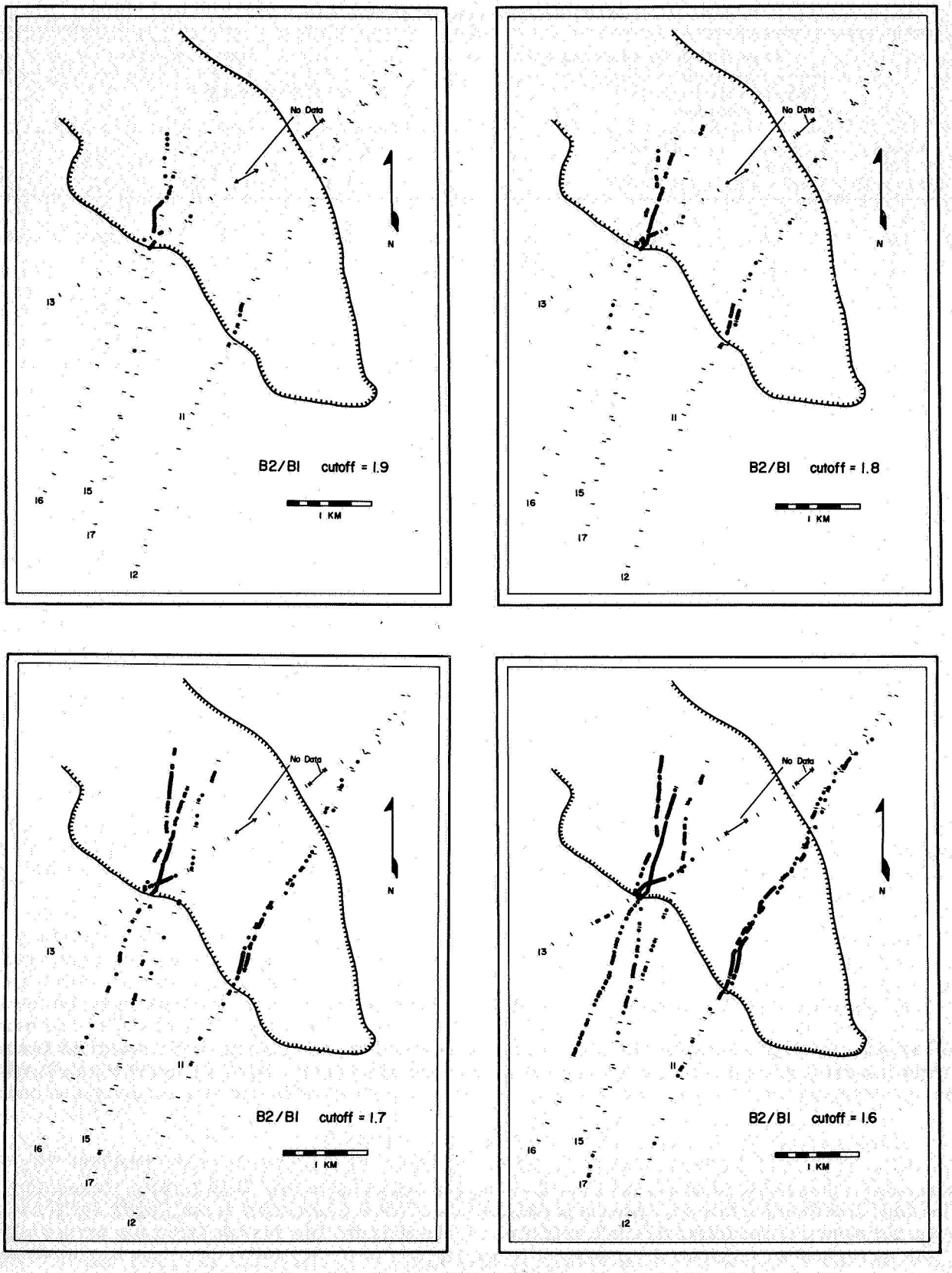

FIG. 7. Plot of anomalous spectra (dots) for different B2/B1 cutoff values for data of September 25, 1978. Symbols same as in Figure 5.

Whereas obvious vegetation density changes do not correlate with our pattern of anomalous spectra, it is possible that subtle density differences occur. On the basis of both laboratory- and field-measured reflectance data collected from Cu-stressed ponderosa pine, Howard et al. (1971) conclude that the stress on the vegetation is manifested primarily as a needle density difference and not a pigment absorption difference. Their basis for this conclusion was that significant differences between the foliage from trees in mineralized and nonmineralized sites were observed only in field measurements, not laboratory measurements where needles were removed from the branches for analysis. A decrease in vegetation density increases the contribution of radiance reflected by the undercover and the ground. It is expected that this would increase the B2/B1 ratio of the spectrum, particularly to the extent that iron oxide-stained outcrops of hydrothermally altered rock show through. Further, experiments by Lyon and Lanz (1980) with an airborne radiometer using optical filters indicate that our B2/B1 ratio correlates with subtle changes in grass patterns and the standard Landsat biomass indicator (Landsat MSS bands (7−5/7+5)). This experiment over grass does not directly relate to forested areas, but it does give an indication that we might be detecting density differences.

Factors other than geochemical stress alone may affect the density of a plant canopy and provide important information for the exploration geologist. For instance, Canney et al. (1979) report that insect infestations and plant diseases may preferentially attack trees in mineralized areas because their vigor is already affected by the anomalous geochemical environment of the soil. Therefore, any canopy density anomaly, even those clearly related to insect infestations, may be ultimately correlated with mineralization.

Another possible cause of a change in the reflectance properties of a plant canopy is a change in the distribution of the species within the canopy. At Mesatchee Creek, the predominant tree type is Douglas fir, but lesser amounts of western larch are interspersed. These two species are commonly associated east of the Cascade Divide (Franklin and Dyrness, 1973; Mosher and Lunnam, 1974). While we saw no obvious correlation between the mineralization and the relative proportions of these two tree types, changes in their relative proportions could exist and be the result of geochemical factors in the soil. Further, since western larch is a deciduous tree, its needles change color and drop in the fall. It is possible, therefore, that either premature senescence of the larch due to a geochemical stress or a simple change in the relative proportions of the two tree species could lead to the observed reflected radiance anomaly (J. Craig McFarlane, pers. commun.).

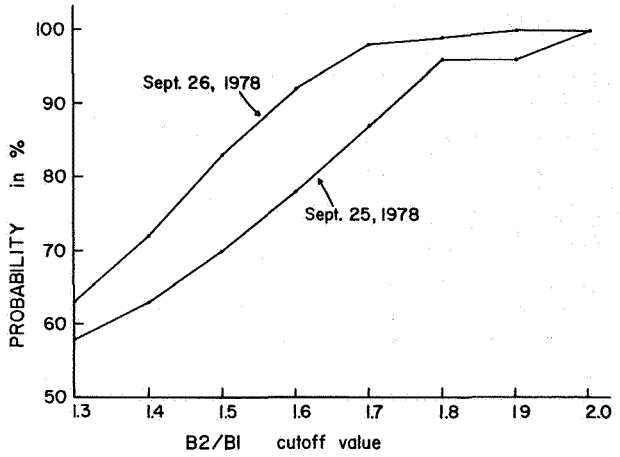

FIG. 8. Plot of B2/B1 cutoff value vs probability (%) that an anomalous spectrum falls in pyrite halo. Based on data in Tables 1 and 2.

The actual geochemical feature of the soil that produces the geobotanical anomaly is not known, but we speculate that, since the anomalous spectra are clearly associated with the pyrite halo, it is a function of soil pH and due to the acid conditions of soil derived from rocks in the pyrite halo. Black (1968, p. 338) reported that Cu toxicity in soil increases as the pH of the soil decreases. Press (1974) supports this conclusion and notes that only under low pH conditions are the metals released to the roots to induce their toxic effects on the vegetation. Although Billings (1950) reported a dramatic geobotanical anomaly in soils derived from hydrothermal altered and pyritized rock in the western Great Basin, he was unable to ascertain whether low pH or certain elemental deficiencies were the cause. The solubility and mobility of molybdenum also increase with decreasing pH, and its toxicity is much greater in low pH soils (Carlisle and Cleveland, 1958). It is possible that the soil geochemical anomaly may extend below the surface within the pyrite halo, and the roots of the trees may tap this subsurface copper source which was not detected by the surface geochemical study, but we have no evidence for this.

There are three significant points that should be emphasized as a conclusion to this study.

First, the experiment suggests that an airborne multispectral scanner of the type used in this study (Chiu and Collins, 1978) can detect geobotanical anomalies that indicate zones of porphyry copper mineralization. This observation supports the earlier work of Birnie and Hutton (1976), Collins et al. (1977, 1978), and Birnie and Dykstra (1978). Analysis of our data indicates that if drill sites had been chosen on the basis of the reflected radiance anomalies, the mineralization would have been discovered.

Secondly, the vegetation present in an area controls

the spectral region in which the geobotanical anomaly is manifested. Experiments on lodgepole pine (Birnie and Hutton, 1976; Birnie and Dykstra, 1978) were undertaken at the Heddleston porphyry copper deposit in Montana. The anomaly in the lodgepole pine appeared in the 670-nm region of the spectrum, which is in the center of one of the chlorophyll absorption bands. The present study indicates that Douglas fir responds at 565 nm at the height of the green peak between chlorophyll absorption bands. Further work must be undertaken to determine the response of other types of vegetation under geologic conditions.

Thirdly, the geochemical feature producing the geobotanical anomaly is associated with the pyrite halo and not restricted to the anomalous soil geochemical zone.

It is clear that more work should be done to determine the botanical processes that produce the geobotanical anomalies and to determine the spectral responses of more and different kinds of vegetation in different geologic settings. However, the remote sensing technique of the sort described in this paper provides the geologist with an additional geophysical tool for prospecting. Remote detection of geobotanical anomalies is no panacea, and it alone will not find mines. However, remote detection of geobotanical anomalies by means of their anomalous reflected radiance patterns does provide a geophysical technique that should be used in the company of other techniques to aid the exploration geologist.

Acknowledgments

This study was supported by NASA Grant NSG 5014. The work could not have been completed without the cooperation and support of the NASA Goddard Institute for Space Studies (GISS), New York, which provided the instrumentation, computer facilities, and some of the computer programs used in the study. Robert Jastrow and Stephen Ungar of GISS made particularly valuable contributions to the study. We are indebted to Duval International, particularly Victor F. Hollister, for providing the ground truth and permitting access to the Mesatchee Creek Prospect. William Hemphill of the U. S. Geological Survey and J. Craig McFarlane of the U. S. Environmental Protection Agency provided important insights into our interpretations. Numerous people at Dartmouth College helped the study and these include Michael Hutton, Peter A. Cohen, Anna Burack, Martha Jean Eger, Betty Stroock, and Carl Baum. Judy Zimicki of Dartmouth provided important input into the botanical aspects of the study. William Collins of Columbia and Robert Layman of Dartmouth are responsible for the successful functioning of the spectroradiometer. Half Zantop of Dartmouth reviewed the manuscript.

September 11, 1979; September 4, 1980

REFERENCES

Billings, W. D., 1950, Vegetation and plant growth as affected by chemically altered rocks in the western Great Basin: Ecology, v. 31, p. 62–74.

Birnie, R. W., and Dykstra, J. D., 1978, Application of remote sensing to reconnaissance geologic mapping and mineral exploration: Remote Sensing Environment Internat. Symposium, 12th, Univ. Michigan, Proc., p. 795–804.

Birnie, R. W., and Hutton, M. S., 1976, Reflectance spectra of vegetation growing over the Heddleston copper-molybdenum deposit, Montana [abs.]: Geol. Soc. America, Abstracts with Programs, v. 8, p. 779–780.

Black, C. A., 1968, Soil-plant relationships, 2nd ed.: New York, Wiley and Sons, 792 p.

Bølviken, B., Honey, F., Levine, S. R., Lyon, R. J. P., and Prelat, A., 1977, Detection of naturally heavy-metal-poisoned areas by Landsat-1 digital data: Jour. Geochem. Explor., v. 8, p. 457–471.

Brooks, R. R., 1972, Geobotany and biogeochemistry in mineral exploration: New York, Harper and Row, 290 p.

Canney, F. C., Yost, E., and Wenderoth, S., 1970, Relationship between vegetation reflectance spectra and soil geochemistry: New data from Catheart Mountain, Maine, *in* Third Annual Earth Resources Program Review: Houston, Texas, NASA MSC-03742, v. 1, p. 18-1–18-9.

Canney, F. C., Cannon, H. L., Cathrall, J. B., and Robinson, K., 1979, Autumn colors, insects, plant disease, and prospecting: ECON. GEOL., v. 74, p. 1673–1676.

Cannon, H. L., 1960, Botanical prospecting for ore deposits: Science, v. 132, no. 3427, p. 591–598.

——1971, The use of plant indicators in ground water surveys, geologic mapping, and mineral prospecting: Taxon, v. 20, p. 227–256.

Carlisle, D., and Cleveland, G. B., 1958, Plants as a guide to mineralization: California Div. Mines Spec. Rept. 50, 31 p.

Chang, S. H., and Collins, W., 1980, Toxic effect of heavy metals on plants [abs.]: Pecora Symposium Exposition, 6th, Sioux Falls, South Dakota, 1980, Program, p. 122–124.

Chiu, H. Y., and Collins, W., 1978, A spectroradiometer for airborne remote sensing: Photogrammetric Engineering, Remote Sensing, v. 44, p. 507–517.

Collins, W., 1978a, Analysis of airborne spectroradiometric data and the use of LANDSAT data for mapping hydrothermal alteration: Geophysics, v. 43, p. 967–987.

——1978b, Remote sensing of crop type and maturity: Photogrammetric Engineering, Remote Sensing, v. 44, p. 43–55.

Collins, W. E., Raines, G. L., and Canney, F. C., 1977, Airborne spectroradiometer discrimination of vegetation anomalies over sulfide mineralization—a remote sensing technique [abs.]: Geol. Soc. America, Abstracts with Programs, v. 9, p. 932–933.

——1978, Airborne spectroradiometer detection of heavy-metal stress in vegetation canopies [abs.]: IAGOD Symposium, 5th, Snowbird, Utah, August, 1978, Programs and Abstracts.

Czehura, S. J., 1977, A lichen indicator of copper mineralization Lights Creek district, Plumas County, California: ECON. GEOL., v. 72, p. 796–803.

Dykstra, J. D., and Birnie, R. W., 1979, Reconnaissance geologic mapping in the Chagai Hills, Baluchistan, Pakistan, by computer processing of Landsat digital data: Am. Assoc. Petroleum Geologists Bull., v. 63, p. 1490–1503.

Franklin, J. F., and Dyrness, C. T., 1973, Natural vegetation of

Oregon and Washington: U. S. Dept. Agriculture Forest Service Gen. Tech. Rept. PNW-8, 417 p.

Fraser, R. S., Gaut, N. E., Reigenstein, E. C., III, and Sievering, H., 1975, Interaction mechanisms—within the atmosphere, *in* Reeves, R. G., ed., Manual of remote sensing, Vol. 1: Am. Soc. Photogrammetry, p. 181–233.

Girling, C. A., Peterson, P. J., and Warren, H. V., 1979, Plants as indicators of gold mineralization at Watson Bar, British Columbia, Canada: ECON. GEOL., v. 74, p. 902–907.

Hollister, V. F., 1978, Geology of the porphyry copper deposits of the western hemisphere: New York, Am. Inst. Mining Metall. Petroleum Engineers, 219 p.

Horler, D. N. H., Barber, J., and Blackman, R. A., 1980, Effects of metal stress on optical properties of plants [abs.]: Pecora Symposium Exposition, 6th, Sioux Falls, South Dakota, 1980, Program, p. 124–126.

Howard, J. A., Watson, R. D., and Hessin, T. D., 1971, Spectral reflectance properties of *Pinus ponderosa* in relation to copper content of the soil—Malachite mine, Jefferson County, Colorado: Remote Sensing Environment Symposium, 7th, Univ. Michigan, 1971, Proc., p. 285–297.

Knipling, E. B., 1970, Physical and physiological basis for the reflectance of visible and near-infrared radiation from vegetation: Remote Sensing Environment, v. 1, p. 155–159.

Lyon, R. J. P., 1975, Correlation between ground metal analysis, vegetation reflectance, and ERTS brightness over a molybdenum deposit, Pine Nut Mountains, Western Nevada: Remote Sensing Environment Internat. Symposium, 10th, Univ. Michigan, 1975, Proc., p. 1031–1041.

Lyon, R. J. P., and Lanz, K., 1980, Airborne geobotany: a data collection system for exploration of biogeochemical and biomass anomalies [abs.]: Pecora Symposium Exposition, 6th, Sioux Falls, South Dakota, 1980, Program, p. 127–130.

Moen, W. S., 1969, Analyses of stream sediment samples in Washington for copper, molybdenum, lead, and zinc: Washington Div. Mines Geology, open-file rept., 4 p.

Mosher, M. M., and Lunnum, K., 1974, Trees of Washington: Pullman, Washington State Univ., Coop. Ext. Service College Agriculture, Bull. 440, 40 p.

NASA, 1968, Application of biogeochemistry to mineral prospecting, a survey: Washington, Natl. Aeronautics Space Adm. NASA SP-5056, 135 p.

Press, N. P., 1974, Remote sensing to detect the toxic effects of metals on vegetation for mineral exploration: Remote Sensing Environment Internat. Symposium, 9th, Univ. Michigan, 1974, Proc., p. 2027–2038.

Press, N. P., and Norman, J. W., 1972, Detection of orebodies by remote-sensing the effects of metals on vegetation: Inst. Mining Metallurgy Trans., v. 81, sec. B, p. B166–168.

Reynolds, C. D., Havryluk, I., Bastamen, S., and Atmowidjojo, S., 1973, The exploration of the nickel laterite deposits in Irian Barat, Indonesia: Geol. Soc. Malaysia Bull. 6, p. 309–323.

Rose, A. W., Hawkes, H. E., and Webb, J. S., 1979, Geochemistry in mineral exploration, 2nd ed.: New York, Academic Press, 657 p.

Rowan, L. C., Wetlaufer, P. H., Goetz, A. F. H., Billingsley, F. C. and Stewart, J. H., 1974, Discrimination of rock types and detection of hydrothermally altered areas in south-central Nevada by the use of computer-enhanced ERTS images: U. S. Geol. Survey Prof. Paper 883, 35 p.

Schmidt, R. G., 1975, Exploration for porphyry copper deposits in Pakistan using digital processing of ERTS-1 data: U. S. Geol. Survey Open-File Rept. 75–18, 26 p.

Schmidt, R. G., and Bernstein, R., 1977, Evaluation of improved digital processing techniques of Landsat data for sulfide mineral prospecting, *in* Proc. of the First Annual William T. Pecora Memorial Symposium, October, 1975, Sioux Falls, South Dakota: U. S. Geol. Survey Prof. Paper 1015, p. 201–212.

Simmons, G. C., Van Noy, R. M., and Zilka, N. T., 1974, Mineral resources of the Cougar Lakes-Mt. Aix study area, Yakima and Lewis counties, Washington: U. S. Geol. Survey Open-File Rept. 74–243, 80 p.

Yost, E., and Wenderoth, S., 1971, The reflectance spectra of mineralized trees: Remote Sensing Environment Symposium, 7th, Univ. Michigan, 1971, Proc., p. 269–284.